INTERNATIONAL JOURNAL OF PRECISION ENGINEERING AND MANUFACTURING Vol. 19, No. 1, pp. 143-154 JANUARY 2018 / 143

REGULAR PAPER

DOI: 10.1007/s12541-018-0017-z
ISSN 2234-7593 (Print) / 2005-4602 (Online)

Three Degree of Freedom Acoustic Energy Harvester Using Improved Helmholtz Resonator

Izhar[1,#] **and Farid Ullah Khan**[2]

1 Department of Mechanical Engineering, CECOS University of IT and Emerging Sciences, Peshawar, Pakistan
2 Institute of Mechatronics Engineering, University of Engineering and Technology, Peshawar, Pakistan
Corresponding Author / E-mail: izhar@cecos.edu.pk

KEYWORDS: Acoustic energy, Conical helmholtz resonator, Energy harvester, Piezoelectric, Three degree of freedom, Wireless sensor node

This paper presents the development of a broadband, multi-frequency acoustic energy harvester. The devised energy harvester contains an optimized Helmholtz resonator with conical cavity and a piezoelectric composite plate. The shape and dimensions of the resonator are selected based on the 3D pressure acoustics analysis in COMSOL Multiphysics®. In addition, a cantilever beam, made up of a brass base, a copper rod and a steel sheet, is integrated with the harvester's piezoelectric plate to add an extra degree of freedom to the device. The developed harvester exhibited three peaks at 1501, 1766 and 1890 Hz frequencies, which correspond to the three resonant frequencies of the harvester. Furthermore, the harvester, when subjected to 130 dB sinusoidal SPL and 1501 Hz resonant frequency, generated a maximum power of 214.23 μW. However, when the harvester is operated under random (real) SPL in the vicinity of household electric generated, it produced about 250 and 265 mV output AC and DC voltage levels respectively.

Manuscript received: February 27, 2017 / Accepted: July 21, 2017

NOMENCLATURE

C = Speed of sound
d_o = Orifice diameter
D_c = Diameter of Helmholtz cavity
F_n = Resonant frequency of Helmholtz resonator
k_a = Stiffness of air residing in Helmholtz cavity
L_o = Length of orifice
m_a = Air mass at orifice
P_a = Acoustic pressure near orifice
P_c = Acoustic pressure inside Helmholtz cavity
P_L = Power delivered to load
R_L = Load Resistance
V_L = Load voltage

1. Introduction

The development in microelectronics and microelectromechanical systems technologies made wireless sensor nodes (WSNs) as one of the vital components in autonomous and intelligent systems. Nowadays, WSNs are broadly employed in personal tracking and recovery systems, aircraft engine sensing and monitoring, wearable biomedical devices, military assets tracking, environmental monitoring, condition monitoring of machinery and structural health monitoring of buildings and civil infrastructures.[1,2] The function of WSN is to sense a physical change (for instance, temperature, pressure, humidity, or acceleration etc.) of the monitoring system and communicate its condition to a control room using wireless transmission.[3] Fig. 1 depicts the layout of a typical WSN. Usually, a WSN is comprised of an antenna, a transmitter, a receiver, a microcontroller, signal conditioning circuit, onboard memory, power management circuit and a sensor. To meet the power requirements of the different parts of the WSN batteries are employed.

In Table 1, the power requirements of commercially available low power WSNs are listed. For the operation of these WSNs, the voltage requirements ranges from 1.8 V to 12 V, however, the electrical current drawn by these devices range from 0.1 μA to 30 mA. Overall, these commercial WSNs consumed power that range from 1.8 μW to 90 mW. Among these WSN s, the maximum power consumption (7.2 to 90 mW) is reported for the wireless carbon monoxide sensors. On the

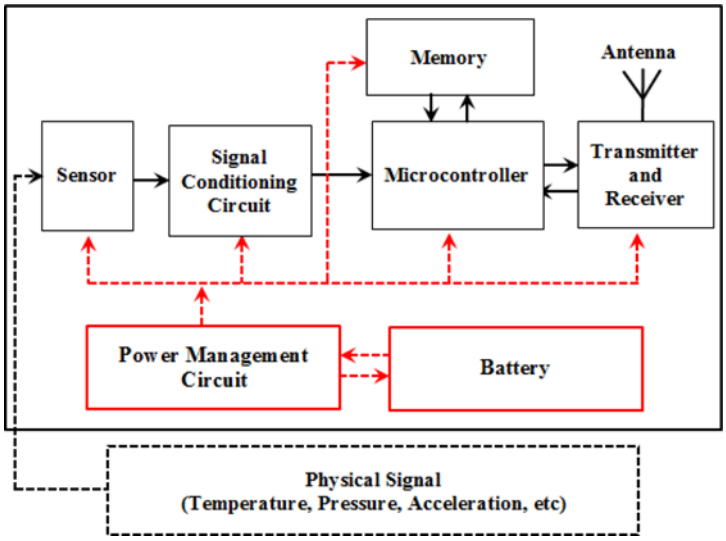

Fig. 1 Block diagram of WSN

Table 1 Electric power consumptions of commercial low power wireless sensors

Sensor type	Model	Manufacturer	Voltage (V)	Current (μA)	Maximum Power (μW)
Humidity	MNS-9-W1-HU-RH	Monnit Co., Utah, US	3	-	80
	HIH-4030/31	Honeywell Inter-national Inc., North Minneapolis	5.8	200	1160
	MNS-9-IN-HU-RH	Monnit Co., Utah, US	3	-	80
Temperature	MCP9700/9700A	Microchip Technology Inc., Arizona, USA	5.5	12	66
	aSM121	Andigilog sensors Inc., Arizona, US	2.7	14	37.8
	TS10	Andigilog sensors Inc., Arizona, US	2.4	12	28.8
	STLM20	STMicroelectronics, Geneva, Switzerland	2.4	4.8	11.52
Smoke	A5367	Allegro MicroSystems, LLC, Massachusetts, USA	12	12	144
	RE46C190	Microchip Technology Inc., Shanghai, China	3	0.1	0.3
Humidity and temperature	HDC1000	Texas Instruments Inc., Dallas, Texas	5	1.2	6
Carbon monoxide	MD036	Monnit Corp., Midvale, Utah	3.6	2000	7200
	EL2764	Risco Group, Midelton, England	3	30000	90000
Acceleration	KXSD9-1026	Kionix Inc., Ithaca, New York	1.8	120	216
	SMB455	Bosch Security Systems, Inc., US	3.3	8000	26400
	MMA1270KEG	Freescale Semiconductor, Inc., Austin, US	5	2100	10500
	ADXL210JQC	Analog Devices, Inc., Massachusetts, US	4.5	600	2700
	MMA7260QT	Freescale Semiconductor, Inc., Austin, US	3.3	500	1650
Pressure	MS5607-B	Measurement Specialties, Ltd., US	1.8	1	1.8
	SCP1000	VIT Technologies, Finland	2.4	3.5	8.4
	BMPO85	Bosch Security Systems, Inc., US	1.8	3	5.4

other hand, the power requirement of the wireless pressure sensors (1.8 to 8.4 μW) reported in Table 1 is minimal. Moreover, the power needs of other wireless sensors, for instance humidity and acceleration, are also relatively high. However, for WSNs, such as, temperature and smoke detector the power consumption is on the lower side (11.52 to 144 μW).

The life time of batteries used to meet the power needs of WSNs are limited. Therefore, batteries have to be recharged or replaced after depletion.[4,5] This actually, confines the usage of WSNs in systems where repeated batteries changeover or recharging in not possible (for instance, in implanted, hazardous, abandoned, embedded, harsh and remote systems). In addition, these depleted batteries causes threat to the environment as these are chemically toxic and required a standard procedure for disposal. In WSNs, the working duration of batteries can be prolonged by increasing the battery size, however, this is not desirable in micro and meso WSNs. Alternatively, batteries life time can be increased by harvesting the ambient energies (such as, solar, thermal, mechanical vibration, acoustic and wind) available in the vicinity of WSNs.[6,7] In the literature a significant amount of work has been performed to harvest energy from ambient sources using energy harvesters (EHs), such as, solar EH,[8] thermal EH,[9] vibration EH[10] and wind EH.[11] Likewise, acoustic is also ambient energy source that exists in enormous amount in the surrounding of WSNs. Table 2 summarizes the magnitude and frequency range of acoustic energy (noise) produced

Table 2 Ambient acoustic energy sources

Source	Frequency Band (Hz)	Sound Pressure Level (dB)	Ref.
Turbofan engines	20-20k	150	12
Automobile surrounding	1-100	90	13
Small power boats	350-1.2k	150	14
Car air conditioning system	20-20k	71.9	15
Food manufacturing industry	-	111	16
Basic metal industry	-	100	
Machines manufacturing industry	-	120	
Aircraft manufacturing industry	-	105	
Oil production activities in ocean	40-100	135	17
Drilling operation in ocean	10-10k	190	
Marine dredging operations	50-500	180	
Gas Turbine Power Plant	30-8k	114.1	1
Compressed air pneumatic hammer	-	100	16
Electric hammer	-	92	

artificially by various mechanical systems in the environment.

Overall, the sound pressure level (SPL) generated by these sources ranges from 71.9 to 190 dB and the overall frequency band reported in the acoustical noise produced by such sources varies from 20 Hz to 20 kHz. The SPL of acoustical noise generated by systems, such as, turbofan engines (150 dB), small power boats (150 dB), drilling operation in ocean (190 dB) and marine dredging operations (180 dB) is pretty high. On the other hand acoustic energy generated by automobile engine (90 dB), car air conditioning system (71.9 dB) and electric hammer (92 dB) is relatively less in magnitude. Furthermore, the frequency spectrum of acoustic noise produced by turbofan engines (20 Hz to 20 kHz), car air conditioning system (20 Hz to 20 kHz), drilling in ocean (10 Hz to 10 kHz) and gas turbine power plant (30 to 8 kHz) have a relatively wide band. Whereas, a narrow frequency band is reported for sources, such as, automobile surroundings (1 to 100 Hz), oil production activities in ocean (40 to 100 Hz) and marine dredging operations (50 to 500 Hz).

The acoustical noise levels produced by ambient acoustic sources, listed in Table 2, can be converted into electrical power with the help of acoustic energy harvester (AEH). The output electrical energy from AEH can be exploited to prolong the workable life of batteries used in WSNs.

In AEHs, usually an acoustic resonator, for instance, Helmholtz resonator (HR), half-wavelength resonator (HWR) or quarter-wavelength resonator (QWR) and an energy conversion mechanism (such as, electromagnetic or piezoelectric) are used. In AEHs, the resonator intensify the ambient acoustic noise level that impinges on the harvester, whereas, the energy conversion mechanism transforms the amplified acoustical wave into useful electrical energy.

To harvest low frequency acoustical noise, Li et al.[18] developed a piezoelectric based AEH in which a QWR and piezoelectric transduction mechanism are integrated. In the harvester, piezoelectric plates (made of Polyvinylidene fluoride) are placed in a QWR. To achieve optimum power, the natural frequencies of the piezoelectric plates and the QWR are kept the same. The harvester having a low resonant frequency (146 Hz) produced a peak power of 2.2 μW under 110 dB SPL. An AEH made-up of two piezoelectric cantilever beams and a HR is developed by Yang et al.[19] For the developed harvester 38 kΩ internal impedance and two resonant frequencies (174 and 201 Hz) are reported. The bandwidths associated with the resonant frequencies of the harvester are 169-179 Hz and 197-204 Hz respectively. Furthermore, the reported harvester generated an optimum power of 1.43 mW at 100 dB SPL. For aero-acoustics applications, a piezoelectric AEH is developed by Horowitz et al.[12] In the harvester, a piezoelectric plate having an electrical impedance of 1 kΩ, is integrated with a HR. The reported AEH with an overall size of 2.445 cm^3 exhibited two resonant frequencies and generated 6 pW optimum power. Kimura el al.[20] utilized a novel non-wet etching technique to develop an enhanced piezoelectric plate for AEHs. From the developed single degree of freedom harvester, a peak power of 140 pW is obtained. To develop a broadband AEH, Peng et al.[21] utilized two HRs, a piezoelectric composite plate and a porous brass plate. In the harvester, a piezoelectric plate is attached to the brass plate which is then sandwiched between the two HRs. For the AEH, three resonant frequencies (1.148, 1.24 and 1.358 kHz) are reported. The bandwidths associated with the three resonant frequencies of the harvester are 1132-1166 Hz, 1232-1246 Hz and 1349-1369 Hz respectively. The overall volume of the harvester is 735.652 cm^3 and it produced a maximum power of 7.5 μW. Lai et al.[22] developed an electromagnetic based AEH that is composed of a permanent magnet, a planar coil and a suspension plate. The harvester having a single resonant frequency of 470 Hz generated an output voltage of 0.24 mV. An electromagnetic based AEH comprised of a HR, a copper wound coil attached to a flexible membrane and a fixed magnet is manufactured by Khan and Izhar.[23] The reported harvester having single resonant frequency (319 Hz) produced an optimum power of about 789 μW. Furthermore, for the harvester the bandwidth 85 Hz (from 240-325) is reported. To produce high power levels, Khan and Izhar[2] reported a hybrid AEH utilizing both electromagnetic and piezoelectric conversion. The developed harvester is consisted of a HR, a bimorph piezoelectric plate sandwiched between two neodymium (NdFeB) magnets and a static copper wound coil. The harvester having an overall volume of about 21 cm^3 generated 52.16 μW power. Furthermore, two resonant frequencies (1 and 2.1 kHz) are reported for the harvester. Moreover, the bandwidths associated with the two resonant frequencies of the harvester are 998-1008 Hz and 2085-2109 Hz respectively.

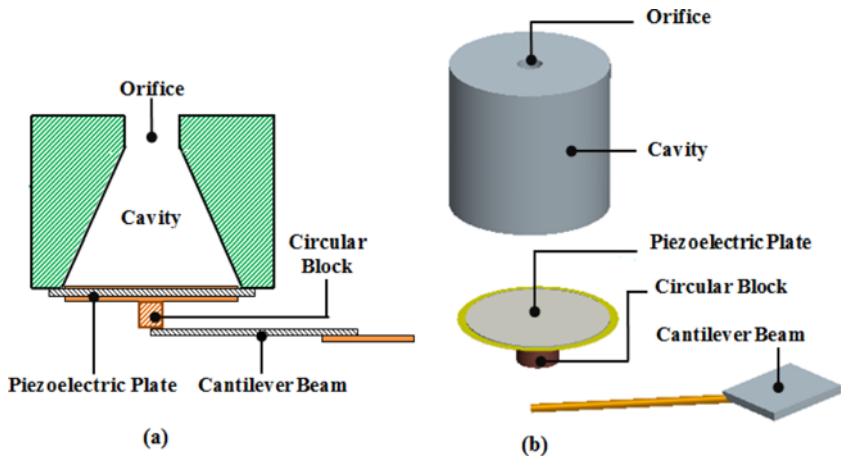

Fig. 2 Developed AEH (a) cross-sectional view and (b) exploded view

Most of the previously fabricated and reported AEHs are narrow band, having one or two resonant frequencies.[2,19,20,22-35] The performance of energy harvester can be enhanced with multi-resonant nature of the device and by widening its frequency bandwidth. This is due to the reason that the frequency band of acoustical noise produced by acoustic sources, as listed in Table 2, is broad and ranges from 1 Hz to 20 kHz. In addition, most of the AEHs reported in the literature utilized a HR with cylindrical shaped cavity to magnify the incoming acoustical noise.[19,29,32,33] A very little research is reported in the literature regarding the optimization of the HR for enhanced performance.

In this work a wideband, three degree of freedom AEH is developed. In the develop harvester, an optimized HR with a conical shape cavity and a bimorph piezoelectric composite plate is used. The shape and dimension of the optimized HR is selected based on the 3D pressure acoustic analysis in COMSOL Multiphysics®. Furthermore, in the harvester, a cantilever beam (made of a brass base, a copper rod and a steel plate) is attached to piezoelectric plate in order to add another resonant frequency and broaden the frequency bandwidth of the device.

2. Operational Mechanism of the Harvester

The developed AEH made up of a HR and a piezoelectric composite plate is illustrated in Fig. 2. Moreover, a cantilever beam, consisted of base (circular block), a copper rod and a steel plate, is attached to the central portion of the composite plate in order to add an extra degree of freedom to the AEH. The HR amplifies the acoustic wave that impinges on it.[36,37] The augmented pressure wave strikes the composite plate and produce deflection in it. The oscillating pressure in the HR cavity produces vibration of the piezoelectric plate and causes tension and compression in the piezoelectric layers of the composite plate. Due to this tension and compression actually voltage is induced in each piezoelectric layer. Furthermore, the incident acoustic wave also produces vibration in the cantilever beam which also contributes towards the composite plate deflection and power generation through piezoelectric layers. As the beam is connected to the piezoelectric composite plate, therefore, the vibration from the beam is transmitted to the piezoelectric plate. Moreover, the cantilever beam (having resonant frequency slightly different from HR and the plate) adds an extra resonant frequency to the developed AEH.

3. Modeling and Simulation of HR

The conventional cylindrical HR, as shown in Fig. 3, comprises of an orifice and a cylindrical cavity. During operation, the air residing in the HR's orifice acts as a lumped mass, it moves up and down about the static equilibrium position. However, the air trapped in the HR's cavity behaves like a spring that helps in the movement of lumped air at the orifice. The acoustic wave, with pressure P_a, near the orifice forces the air mass (existing in orifice) into the resonator's cavity. This moves the lumped mass below the equilibrium position and in turn upsurges the cavity's pressure to P_c. The augmented pressure P_c in the cavity then pushes the air mass at the orifice in upward direction. Due to this, the pressure in the cavity declines as the lumped mass is moved slightly above the equilibrium position. Furthermore, due to this low cavity's pressure and high incident pressure P_a, the air mass (at the orifice) is again pushed into the cavity. In the HR this oscillatory movement is continued periodically as long as it is subjected to acoustic pressure wave. A HR can be modeled as a single degree of freedom, mass-spring-damper system as illustrated in Fig. 3. The air (residing in the orifice) has mass and possesses kinetic energy, which can be modeled as lumped mass m_a. In addition, the air existing in the resonator's cavity acts like a spring (with stiffness k_a), pulling and pushing the air mass m_a at the orifice. Furthermore, the orifice offers resistance to the air as it oscillates in it. The resistive loss in the orifice is represented by damping coefficient c_a in the lumped parameter model as shown in Fig. 3(b). For the lumped parameter model of the HR the undamped natural frequency[38]

$$F_n = \frac{C}{2\pi}\sqrt{\frac{3d_o^2}{4D_c^2 L_o L_c}} \tag{1}$$

can be derived in terms of sound speed C, orifice diameter d_o and length L_o, and cavity diameter D_c and length L_c. Eq. (1) can be used to design and tune a HR for a desired natural frequency.

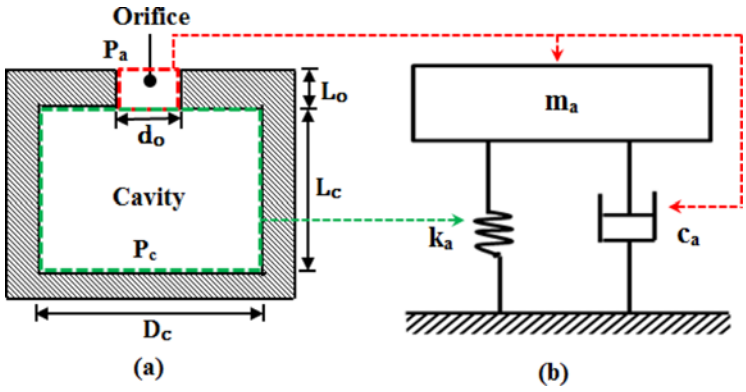

Fig. 3 HR: (a) Cross-sectional view and (b) Lumped parameter model

Table 3 Dimensions of simulated HRs

Description		Value	
		HR with cylindrical cavity (mm)	HR with conical cavity (mm)
Orifice	Height	7	7
	Diameter	5	5
Cavity	Height	16	16
	Base Diameter	20	20

In most of the reported AEHs conventional HR with cylindrical cavity, as shown in Fig. 3(a), are used. In this work HR with conical shaped cavity is modeled and simulated in COMSOL Multiphysics®. Moreover, the simulation results of the HR with conical cavity are also compared with conventional HR.

To model the HRs in COMSOL Multiphysics®, 3-D pressure acoustics (frequency domain analysis) is utilized. In the software, the orifice of HR is set as sound soft and its other boundaries are set as sound hard. In addition, various material properties of air (present in the HR), for instance dynamic viscosity, density, speed of sound (in air) and bulk viscosity are set to 1.98×10^{-04} Ns/m^2, 1.225 kg/m^3, 332 m/s and zero respectively. Moreover, the dimensions of the simulated HRs, as listed in Table 3, are kept similar for comparison. For each HR, initially using eigen frequency study the resonant frequencies are obtained in COMSOL Multiphysics. Next, the frequency response of each HR is plotted for various input SPLs. Finally, the pressure variations inside HRs at their corresponding resonant frequencies are plotted.

In Fig. 4, the frequency response of the simulated HRs in terms of cavity's pressure at different SPLs is shown. Single peak, as depicted in Fig. 4(a), is observed at 1118 Hz frequency which corresponds to the resonant frequency of the HR with cylindrical cavity. Similarly, in Fig. 4(b), peak is observed at 1538 Hz frequency, which is actually the resonant frequency of HR with conical cavity. Furthermore, it is quite evident from the Figure that under similar input SPL (130 dB), the pressure (201 dB) produced in the cavity of the HR with conical shape is comparatively greater than HR with cylindrical cavity (194 dB).

The pressure variation inside the HRs at their corresponding resonant frequencies is also simulated in COMSOL Multiphysics®. During the simulation, the resonators are excited, at 130 dB SPL and at their corresponding resonant frequency. The pressure variation inside each HR's cavity is shown in Fig. 5. It is obvious from the Figure that in each resonator, the pressure along its longitudinal axis increases from the orifice to the bottom. Furthermore, the maximum SPL is reported in the HR with conical shape, which actually is 201 dB in magnitude.

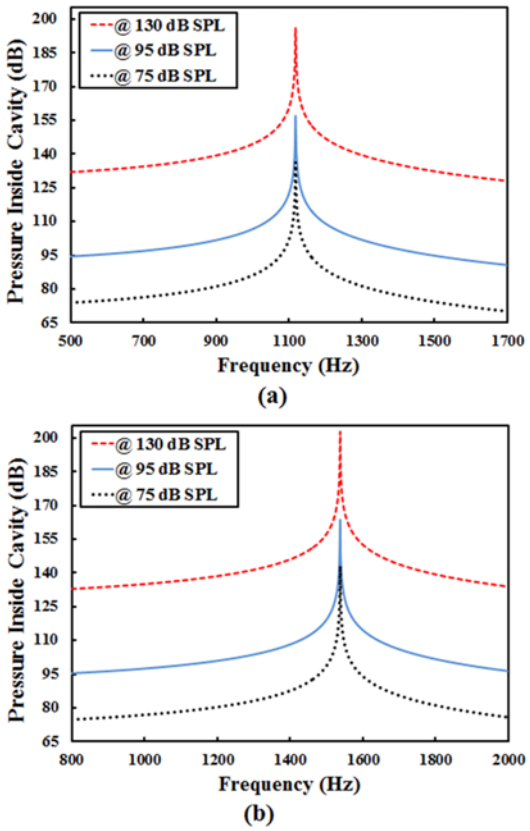

Fig. 4 Frequency response of the resonators in terms of their cavity's pressure: (a) Conventional HR with cylindrical cavity and (b) HR with conical cavity

4. Fabrication of the Prototypes

For the fabrication of HR with conical cavity, Teflon (Shandong

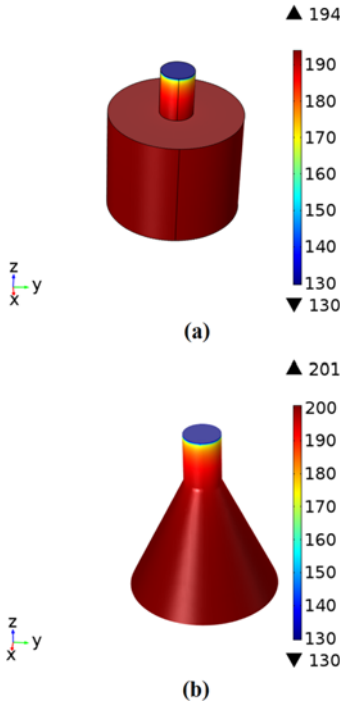

Fig. 5 Pressure variation inside the resonators along their longitudinal axis: (a) HR with cylindrical cavity and (b) HR with conical cavity

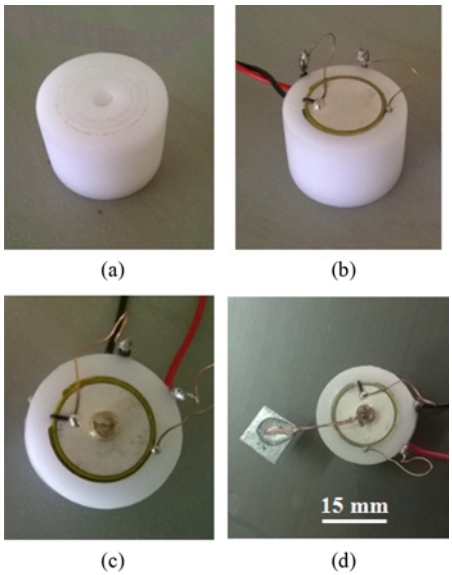

Fig. 6 Fabrication of prototype: (a) HR (b) Piezoelectric plate bonded onto HR (c) Circular block (brass) attached to the piezoelectric plate (d) Cantilever beam glued to the base block

Senrong Plastic Industry Technology Co., Shandong, China) is used, whereas, for base of cantilever beam, brass (Manufacturer's Brass and Aluminum Foundry Inc., Blue Island, Illinois, USA) is utilized. To produce the beam's base and the HRs conventional machining processes are performed on a 1.27 cm brass rod and 2.54 cm Teflon rod respectively. Furthermore, the components of cantilever beam are made from commercial copper rod (Pakistan Cables Co., Karachi, Pak) and steel sheet (KK Steels International Co., Faisalabad, Pak). Moreover, commercially available piezoelectric plate (Disc Benders, Bimorphs, American Piezo Inc., Mill Hall, Pennsylvania, USA), is integrated with the prototype's cavity to convert the HR's oscillations into electrical energy. The plate is composed of a 100 μm thick brass layer which is sandwiched between two 130 μm thick Lead Zirconate Titanate (PZT) layers.

Table 4 Parameters and dimensions of a fabricated AEH

Description			Value
Helmholtz resonator	Orifice diameter		5 mm
	Orifice height		7 mm
	Helmholtz cavity diameter		20 mm
	Helmholtz cavity height		16 mm
Piezoelectric plate	Impedance of piezoelectric plate		1000 Ω
	Piezoelectric constant (d_{33})		290 pm/
	Diameter of brass		21 mm
	Diameter of PZT ceramic		20 mm
	Thickness of brass		100 μm
	Thickness of PZT		260 μm
	Total thickness of plate		360 μm
	Impedance of piezoelectric plate		1000 Ω
Cantilever beam	Copper rod	Length	23 mm
		Diameter	1.25 mm
	Steel plate	Length	12.5 mm
		Width	12.5 mm
	Beam base (Brass Block)	Proof mass	0.84 gram
		Diameter	5 mm
		Height	5 mm

The steps involved in the assembly of the prototype are illustrated in Fig. 6.

First of all, the HR and the bimorph piezoelectric composite plate are attached to each other, Fig. 6(b). The brass cylindrical block, which acts as a base for the cantilever beam, is bonded onto the piezoelectric plate as shown in Fig. 6(c). One end of the copper beam is then joined with the brass block. Finally, the steel plate is attached to the free end of the copper beam, Fig. 6(d). During the assembly of the prototype commercially available superglue (Fixee, Lahore, Pak) is used to assemble the components of the prototype. In Table 4, the parameters and properties of various components of prototype are listed.

5. Experimentation of the Harvesters

The developed prototypes are tested both under harmonic SPL inside laboratory, and random SPL, in real environment in the surrounding of a motorcycle and an electric generator. The setup for the experimentation of prototype under harmonic SPL is illustrated in Fig. 7.

To determine the optimum power generated by the harvester with beam, the harvester is exposed to different sinusoidal acoustic signals (75, 100 and 130 dB SPL) at1501 Hz (first resonant frequency) and a variable load resistance is connected with the harvester and then the resistance is varied from 0 to 4000 Ω. The corresponding load voltage levels are measured and plotted against load resistance as shown in Fig. 9(a). From the root mean square (rms) load voltage (V_L) measurements, the output average power[39]

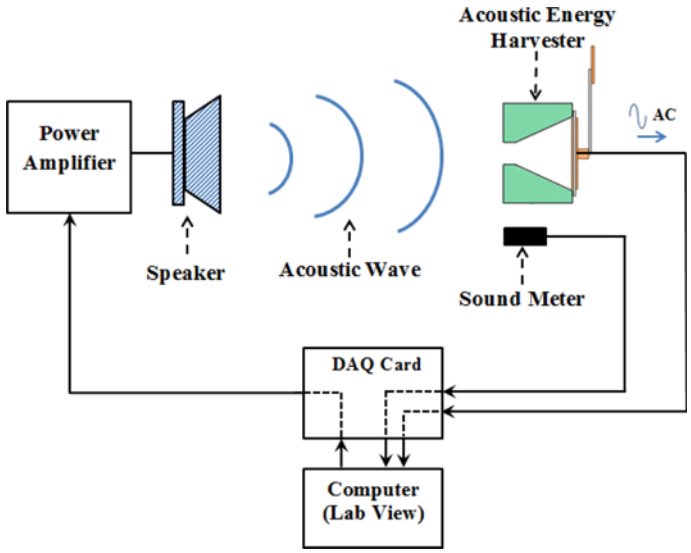

Fig. 7 Block diagram of the experiment equipment

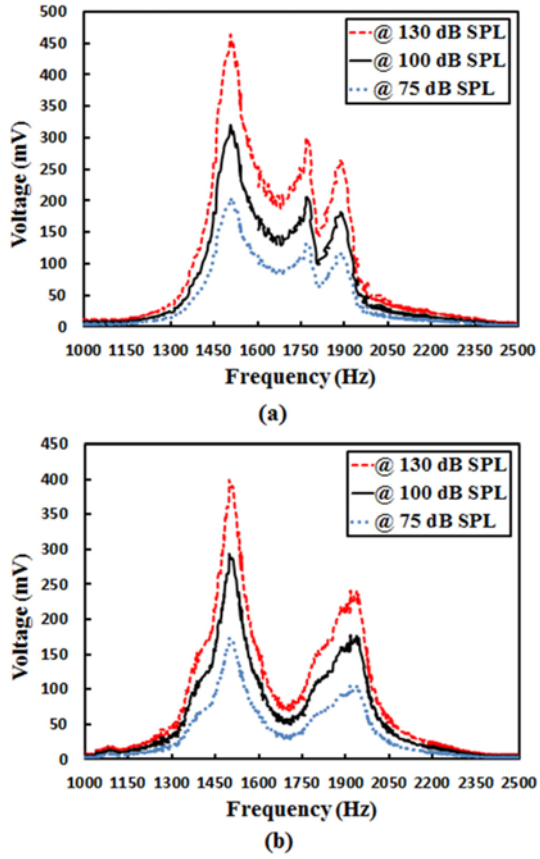

Fig. 8 Load voltage produced by the harvester as a function of frequency when connected to 1 kΩ resistance (a) with beam (b) without beam

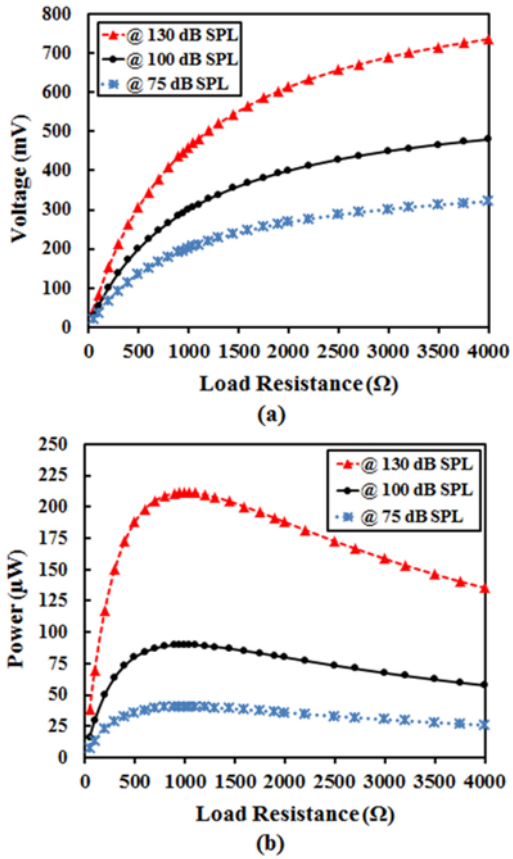

Fig. 9 Output generation of the harvester (a) Load voltage (b) Load power

$$P_L = \frac{V_L^2}{R_L} \tag{2}$$

is computed and plotted as function of load resistance (R_L) as shown in Fig. 9(b). From Fig. 9(b), it is evident that the optimum load resistance for the harvester is 1 kΩ, which is equal to the resistance of the piezoelectric plate (as listed in Table 4). Under optimum load condition, and when exposed to 130 dB SPL, the maximum power transferred to the load resistance, is 214.23 μW.

The voltage produced by the developed harvester is alternating, conversely, the voltage needed for the operation of WSNs is usually

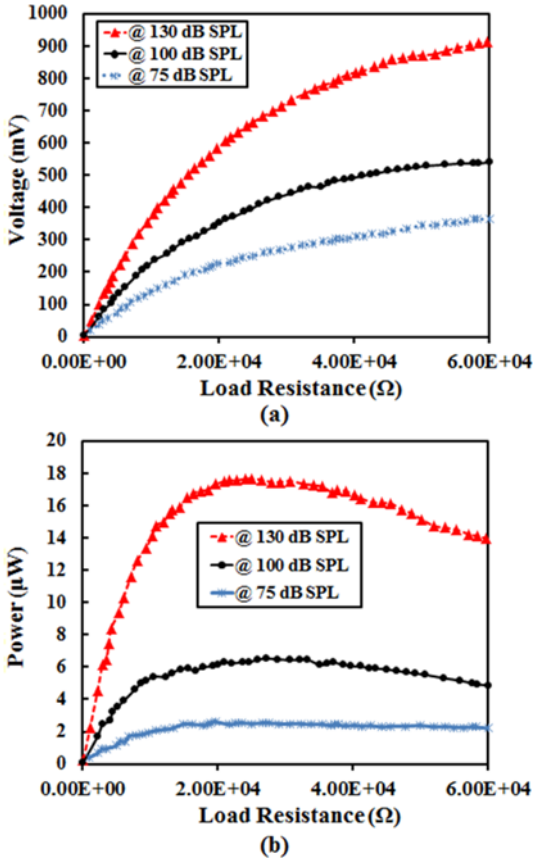

Fig. 10 DC output of the harvester with rectifier (a) Rectified load voltage (b) Load power

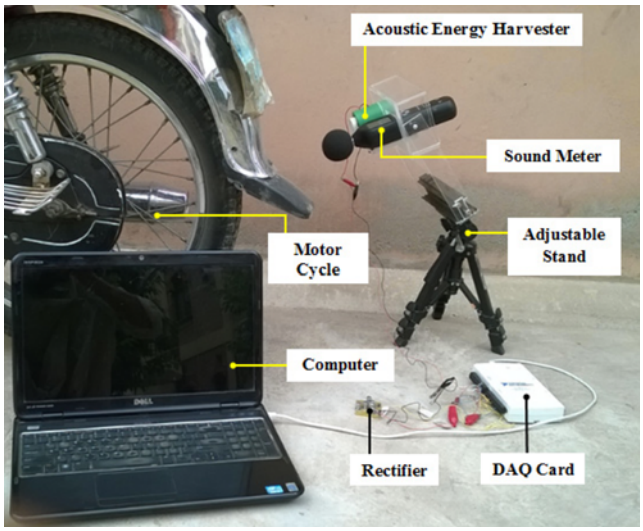

Fig. 11 Testing setup for characterization of AEH in the vicinity of motorcycle

DC. Therefore, the AC voltage from the harvester needs to be converted into DC voltage prior to its supply to the WSN. In order to rectify the AC voltage produced from the harvester, a three stage ultra-low voltage Cockcroft Walton AC to DC converter developed by Khan et al.[40] is connected with the harvester and its response is examined. Figs. 10(a) and 10(b) respectively depicts the rectified load voltage and power

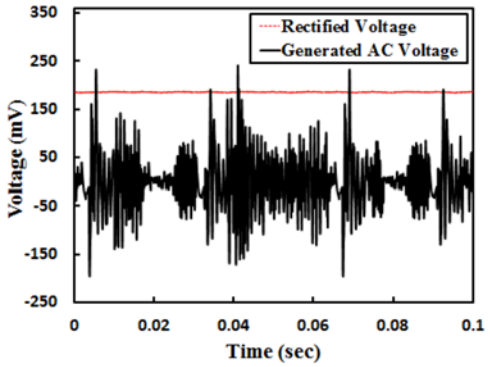

Fig. 12 Time response of the AEH under ambient acoustical noise produced from motorcycle

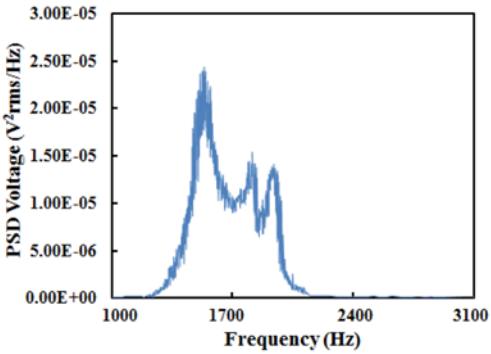

Fig. 13 PSD of output voltage generated by the AEH in the vicinity of motorcycle

produced by the harvester as a function of load resistance. It is obvious from Fig. 10(b) that the optimum load condition for the harvester is altered from 1 kΩ to 2.5 kΩ due to the addition of the rectifier. This is because of the fact that the rectifier's internal impedance also contributes towards the overall impedance and as a result the optimum load condition for the harvester is changed. The maximum power produced by the harvester, with rectifier, is 17.64 μW at 130 dB SPL. This value is relatively less than the power produced (214.23 μW) from the harvester without rectifier. This power reduction is due to the power consumption of the rectification circuit.

To evaluate the performance of the developed harvester under random and chaotic SPL, it is tested in the surrounding of a domestic motorcycle and house hold electric generator. The testing setup for this experimentation is shown in Fig. 11. The setup consists of an adjustable stand holding the AEH and sound meter, a rectifier and LabVIEW software running in the computer.

The response of the AEH in terms of its AC and rectified DC output voltage is illustrated in Fig. 12. From Figure it is clear that the output AC voltage from the harvester is random which is due to chaotic nature of acoustical noise generated by the motorcycle. The random AC output of the harvester exhibit periodic peaks of 248 mV in the time response. However, after rectification the harvester output a DC voltage of 190 mV is produced by the harvester.

The power spectral density (PSD) of output voltage from the AEH is shown in Fig. 13. In the figure three crests are observed (at 1501,

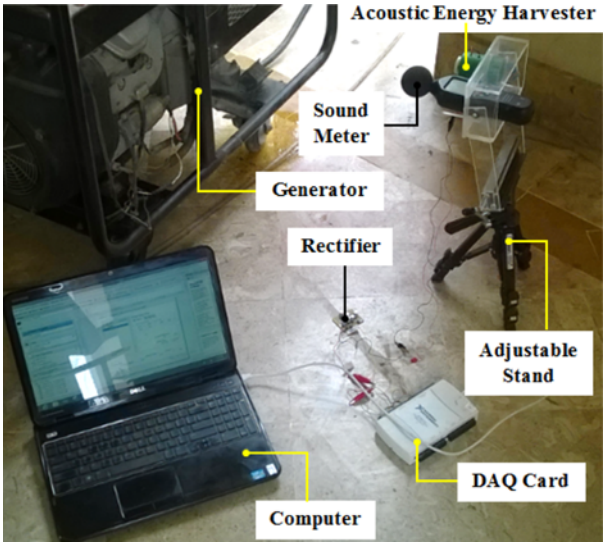

Fig. 14 Experimental setup for testing of the AEH in the vicinity of electric generator

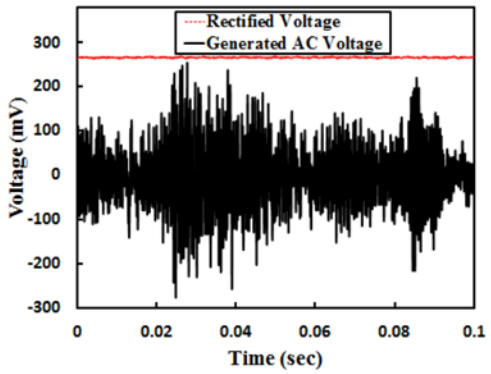

Fig. 15 Time response of the harvester in terms of output voltage in vicinity of electric generator

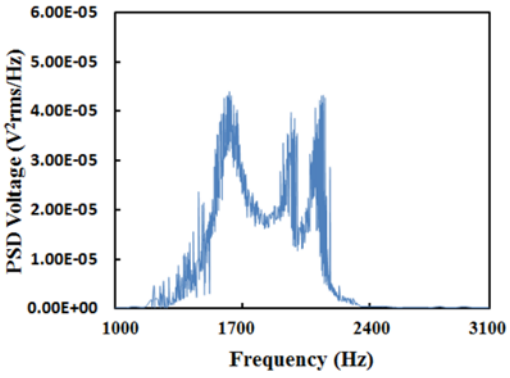

Fig. 16 Frequency response of the AEH in terms of PSD in the vicinity of electric generator

1766 and 1890 Hz) which corresponds to the three resonant frequencies of the harvester. Furthermore, the associated frequency bandwidth for the harvester, as depicted in Fig. 13, ranges from 1453-1542 Hz, 1710-1780 Hz and 1848-1915 Hz. Moreover, the maximum PSD value of

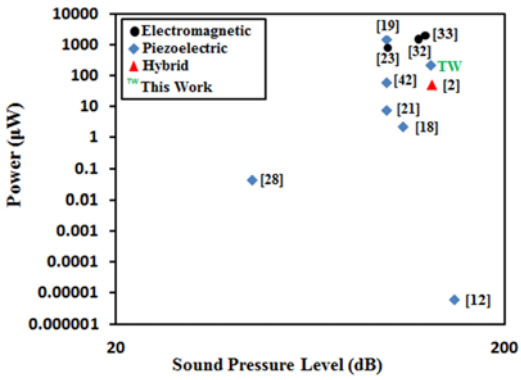

Fig. 17 Power generated by fabricated and reported AEHs versus SPL

about 2.45×10^{-5} V^2/Hz is reported for the harvester at 1501 Hz resonant frequency in this experimentation.

The fabricated AEH is also tested in the vicinity of domestic electrical generator as depicted in Fig. 14. The output AC and rectified voltages generated by the harvester when placed in the vicinity of electric generator is shown in Fig. 15. In this experiment, the AEH produced AC and DC voltages of about 250 and 265 mV respectively. The PSD analysis of the harvester is illustrated in Fig. 16. The bandwidth of the harvester reported in this experiment, as shown in Fig. 16, ranges from 1495-1642, 1740-1795 and 1873-1908 Hz. Furthermore, the maximum PSD value recorded for the developed harvester during this experiment is about 4.3×10^{-05} V^2/Hz.

6. Discussion

The fabricated AEH is compared with the reported AEHs on the basis of various properties (such as, number of resonant frequencies, bandwidth, SPL, size of device, output power and power density) as listed in Table 5. The number of resonant frequencies of the harvester developed in this work are more than all of the reported AEHs except the harvester reported by Peng et al.[21] In addition, the overall bandwidth of the devised harvester in comparison to the reported harvesters is also on the wider side. Furthermore, the resistance of the developed AEH is relatively less than most of the harvesters reported in the literature.

Moreover, the power densities of the developed energy harvesters are much greater than almost all the reported acoustic energy harvesters except the harvester reported by Khan and Izhar.[32]

The power generated by the fabricated and reported AEHs in terms of the SPL is shown in Fig. 17.

The power produced by the developed harvester is pretty greater than most of the reported AEHs and is quite comparable to the harvesters developed by Yang et al.,[19] Khan and Izhar,[23] Khan and Izhar[32] and Khan and Izhar.[33] Furthermore, the overall volume of the developed AEH, as illustrated in Fig. 18, is quite less than all the reported harvesters except the AEHs developed by Horowitz et al.,[12] and Khan and Izhar.[32]

Fig. 19 depicts the power density produced by the AEHs as function of harvester's size. It is clear from the figure that the power density

Table 5 Summary of reported and developed AEHs

Type	Resonant Frequencies	Bandwidth	SP (dB)	Frequency (kHz)	Voltage (mV)	Internal Resistance (Ω)	Power (μW)	Device Size (cm^3)	Power Density ($\mu W/cm^3$)	Ref.
Piezoelectric	2	- - -	149	13.57	- - -	1×10^3	6×10^{-6}	2.445	2.94×10^{-6}	12
	3	1132-1166, 1232-1246 & 1349-1369	100	1.758	- - -	7.5×10^3	7.5	735.652	10.2×10^{-3}	21
	1	- - -	100	16.7	- - -	75	140×10^{-6}	- - -	- - -	20
	1	- - -	100	4.92	- - -	50	82.8×10^{-6}	- - -	- - -	27
	1	- - -	110	0.146	- - -	1×10^6	2.2	1500	1.5×10^{-3}	18
	1	- - -	100	0.242	2000	70×10^3	55	900	61.11×10^{-9}	41
	2	169-179 & 197-204	100	0.201	- - -	38×10^3	1430	3972.22	360×10^{-3}	19
	-	- - -	45	4.2	- - -	3.9×10^3	40×10^{-3}	47.149	8.48×10^{-4}	28
	1	- - -	110	6.28	- - -	56.8	0.68×10^{-6}	- - -	- - -	42
	3	1453-1542, 1710-1780 & 1848-1915	130	1.501	461	1000	214.23	13.12	16.32	This work
Electromagnetic	1	- - -	- - -	0.470	0.24	- - -	- - -	0.009	- - -	22
	1	110-140	120	0.144	- - -	66	1500	7.860	56.6	32
	1	240-325	100	0.319	198.7	50	789.65	13.57	58.19	23
	1	140-148	125	0.143	- - -	52	1960	14.7	133.3	33
Hybrid	2	992-1008 & 2085-2109	130	2.1	481	1142	51.16	21.2	2.45	2

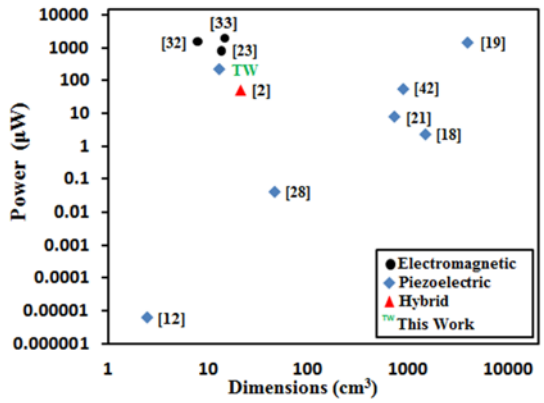

Fig. 18 Power generated by fabricated and reported AEHs versus device dimensions

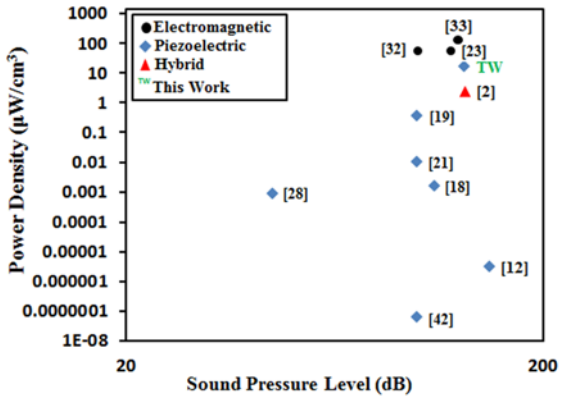

Fig. 19 Power density of the fabricated and reported AEHs versus SPL

generated by the harvester produced in this work is quite higher than most of the reported AEHs and comparable with the harvesters reported by Khan and Izhar,[23] Khan and Izhar[32] and Khan and Izhar.[33]

7. Conclusion

In this work, the development of an acoustic energy harvester (AEH) that employs a Helmholtz resonantor (HR), a piezoelectric composite plate and a cantilever beam is investigated. An optimized HR with conical cavity is utilized in the harvester. The attached cantilever beam (made up of brass base, copper rod and steel sheet), helped in broadening of the frequency bandwidth of the harvester. The devised harvester is characterized both under sinusoidal SPLs inside lab and random SPLs in real environment in the vicinity of ambient acoustic energy sources. When, the harvester is characterized without the cantilever beam. In the harvester's frequency response curve two peaks were observed (at 1501 and 1938 Hz frequencies), which correspond to its two resonant frequencies. In comparison, when the cantilever beam is added to the harvester, the bandwidth of the device is increased and moreover, the AEH exhibited three resonant frequencies (1501, 1766 and 1890 Hz). Furthermore, inside lab, the maximum power produced by the developed AEH is 214.23 μW, when exposed to 130 dB SPL and 1501 Hz frequency. In addition, the maximum AC and DC voltages generated by the developed AEH are 250 and 265 mV respectively, when tested under random SPL produced by the domestic electric generator. In comparison to the reported AEHs, the developed AEH is capable of producing compariable power and power density. Moreover, due to the nature of three degree of freedom of the harvester the frequency bandwidth of the device is also better than most of the reported AEHs.

Furthermore, the power levels generated by the devised AEH are quite enough to operate wireless sensor nodes functioning in acoustical source envirnoment.

REFERENCES

1. Khan, F. U., "State of the Art in Acoustic Energy Harvesting," Journal of Micromechanics and Microengineering, Vol. 25, No. 2, Paper No. 023001, 2015.
2. Khan, F. U. and Izhar, "Hybrid Acoustic Energy Harvesting Using Combined Electromagnetic and Piezoelectric Conversion," Review of Scientific Instruments, Vol. 87, No. 2, Paper No. 025003, 2016.
3. Angelopoulos, C. M., Nikoletseas, S., and Theofanopoulos, G. C., "A Smart System for Garden Watering Using Wireless Sensor Networks," Proc. of the 9th ACM International Symposium on Mobility Management and Wireless Access, pp. 167-170, 2011.
4. Khan, F., Sassani, F., and Stoeber, B., "Copper Foil-Type Vibration-Based Electromagnetic Energy Harvester," Journal of Micromechanics and Microengineering, Vol. 20, No. 12, Paper No. 125006, 2010.
5. Khan, F., Sassani, F., and Stoeber, B., "Nonlinear Behaviour of Membrane Type Electromagnetic Energy Harvester Under Harmonic and Random Vibrations," Microsystem Technologies, Vol. 20, No. 7, pp. 1323-1335, 2014.
6. Zhou, G., Huang, L., Li, W., and Zhu, Z., "Harvesting Ambient Environmental Energy for Wireless Sensor Networks: A Survey," Journal of Sensors, Vol. 2014, Article ID: 815467, 2014.
7. Pillai, M. A. and Deenadayalan, E., "A Review of Acoustic Energy Harvesting," Int. J. Precis. Eng. Manuf., Vol. 15, No. 5, pp. 949-965, 2014.
8. Seo, H., Ichida, D., Uchida, G., Kamataki, K., Itagaki, N., et al., "Analysis on the Photovoltaic Property of Si Quantum Dot-Sensitized Solar Cells," Int. J. Precis. Eng. Manuf., Vol. 15, No. 2, pp. 339-343, 2014.
9. Kang, T. J., Fang, S., Kozlov, M. E., Haines, C. S., Li, N., et al., "Electrical Power from Nanotube and Graphene Electrochemical Thermal Energy Harvesters," Advanced Functional Materials, Vol. 22, No. 3, pp. 477-489, 2012.
10. Kim, G.-W., Kim, J., and Kim, J.-H., "Flexible Piezoelectric Vibration Energy Harvester Using a Trunk-Shaped Beam Structure Inspired by an Electric Fish Fin," Int. J. Precis. Eng. Manuf., Vol. 15, No. 9, pp. 1967-1971, 2014.
11. Truitt, A. and Mahmoodi, S. N., "A Review on Active Wind Energy Harvesting Designs," Int. J. Precis. Eng. Manuf., Vol. 14, No. 9, pp. 1667-1675, 2013.
12. Horowitz, S. B., Sheplak, M., Cattafesta III, L. N., and Nishida, T., "A MEMS Acoustic Energy Harvester," Journal of Micromechanics and Microengineering, Vol. 16, No. 9, pp. S174-S181, 2006.
13. Jung, S. S., Kim, Y. T., Lee, Y. B., Kim, H. C., Shin, S. H., and Cheong, C., "Spectrum of Infrasound and Low-Frequency Noise in Passenger Cars," Journal of the Korean Physical Society, Vol. 55, No. 6, pp. 2405-2410, 2009.
14. Barlett, M. L. and Wilson, G. R., "Characteristics of Small Boat Acoustic Signatures," Vol. 112, No. 5, 2002. (DOI: 10.1121/1.4778778)
15. Yokoyama, Y. and Hashimoto, K., "Development of Low-Noise Air Conditioning Ducts," East Japan Railway Culture Foundation, Vol. 16, pp. 63-66, 2010.
16. Gerges, N. Y., "Noise Sources," http://www.who.int/occupational_health/publications/noise5.pdf (Accessed 28 NOV 2018)
17. Greene, C. and Moore, S., "Man-Made Noise," Marine Mammals and Noise, pp. 101-158, 1995.
18. Li, B., Laviage, A. J., You, J. H., and Kim, Y.-J., "Harvesting Low-Frequency Acoustic Energy Using Quarter-Wavelength Straight-Tube Acoustic Resonator," Applied Acoustics, Vol. 74, No. 11, pp. 1271-1278, 2013.
19. Yang, A., Li, P., Wen, Y., Lu, C., Peng, X., et al., "Note: High-Efficiency Broadband Acoustic Energy Harvesting Using Helmholtz Resonator and Dual Piezoelectric Cantilever Beams," Review of Scientific Instruments, Vol. 85, No. 6, Paper No. 066103, 2014.
20. Kimura, S., Tomioka, S., Iizumi, S., Tsujimoto, K., Sugou, T., and Nishioka, Y., "Improved Performances of Acoustic Energy Harvester Fabricated Using Sol/Gel Lead Zirconate Titanate Thin Film," Japanese Journal of Applied Physics, Vol. 50, No. 6S, Paper No. 06GM14, 2011.
21. Peng, X., Wen, Y., Li, P., Yang, A., and Bai, X., "A Wideband Acoustic Energy Harvester Using a Three Degree-of-Freedom Architecture," Applied Physics Letters, Vol. 103, No. 16, Paper No. 164106, 2013.
22. Lai, T., Huang, C., and Tsou, C., "Design and Fabrication of Acoustic Wave Actuated Microgenerator for Portable Electronic Devices," Proc. of MEMS/MOEMS Symposium on Design, Test, Integration and Packaging of MEMS/MOEMS, pp. 28-33, 2008.
23. Khan, F. U., "Electromagnetic Energy Harvester for Harvesting Acoustic Energy," Sādhanā, Vol. 41, No. 4, pp. 397-405, 2016.
24. Wang, W.-C., Wu, L.-Y., Chen, L.-W., and Liu, C.-M., "Acoustic Energy Harvesting by Piezoelectric Curved Beams in the Cavity of a Sonic Crystal," Smart Materials and Structures, Vol. 19, No. 4, Paper No. 045016, 2010.
25. Liu, F., Phipps, A., Horowitz, S., Ngo, K., Cattafesta, L., Nishida, T., and Sheplak, M., "Acoustic Energy Harvesting Using an Electromechanical Helmholtz Resonator," The Journal of the Acoustical Society of America, Vol. 123, No. 4, pp. 1983-1990, 2008.
26. Horowitz, S. B., "Development of a MEMS-Based Acoustic Energy Harvester," University of Florida, 2005.
27. Iizumi, S., Kimura, S., Tomioka, S., Tsujimoto, K., Uchida, Y., et al,

"Lead Zirconate Titanate Acoustic Energy Harvesters Utilizing Different Polarizations on Diaphragm," Procedia Engineering, Vol. 25, pp. 187-190, 2011.

28. Wu, L.-Y., Chen, L.-W., and Liu, C.-M., "Acoustic Energy Harvesting Using Resonant Cavity of a Sonic Crystal," Applied Physics Letters, Vol. 95, No. 1, Paper No. 013506, 2009.
29. Atrah, A. B. and Salleh, H., "Simulation of Acoustic Energy Harvester Using Helmholtz Resonator with Piezoelectric Backplate," Proc. of the 20th International Congress on Sound and Vibration (ICSV20), pp. 7-11, 2013.
30. Li, B., You, J. H., and Kim, Y.-J., "Low Frequency Acoustic Energy Harvesting Using PZT Piezoelectric Plates in a Straight Tube Resonator," Smart Materials and Structures, Vol. 22, No. 5, Paper No. 055013, 2013.
31. Li, B., Laviage, A. J., You, J. H., and Kim, Y.-J., "Acoustic Energy Harvesting Using Quarter-Wavelength Straight-Tube Resonator," Proc. of ASME 2012 International Mechanical Engineering Congress and Exposition, pp. 467-473, 2012.
32. Khan, F. and Izhar, E., "Acoustic-based Electrodynamic Energy Harvester for Wireless Sensor Nodes Application," International Journal of Materials Science and Engineering, Vol. 1, No. 2, pp. 72-78, 2013.
33. Khan, F. U. and Izhar, "Electromagnetic-based Acoustic Energy Harvester," Proc. of 16th International Multi Topic Conference (INMIC), pp. 125-130, 2013.
34. Tomioka, S., Kimura, S., Tsujimoto, K., Iizumi, S., Uchida, Y., et al., "Lead-Zirconate-Titanate Acoustic Energy Harvesters with Dual Top Electrodes," Japanese Journal of Applied Physics, Vol. 50, No. 9S2, Paper No. 09ND16, 2011.
35. Shinoda, S., Tai, T., Itoh, H., Sugou, T., Ichioka, H., et al., "Lead Zirconate Titanate Acoustic Energy Harvester Proposed for Microelectromechanical System/Ic Integrated Systems," Japanese Journal of Applied Physics, Vol. 49, No. 4S, Paper No. 04DL21, 2010.
36. Rossi, M., "Acoustics and Electroacoustics" Artech House Publishers, 1988.
37. Noh, S., Lee, H., and Choi, B., "A Study on the Acoustic Energy Harvesting with Helmholtz Resonator and Piezoelectric Cantilevers," Int. J. Precis. Eng. Manuf., Vol. 14, No. 9, pp. 1629-1635, 2013.
38. Nolle, A., "Small-Signal Impedance of Short Tubes," The Journal of the Acoustical Society of America, Vol. 25, No. 1, pp. 32-39, 1953.
39. Wangsness, R. K., "Electromagnetic Fields," John Wiley & Sons, 2nd Ed., 1986.
40. Ullah, F., Ali, T., and Jamil, K., "Development of a Low Voltage AC to DC Converter for Meso and Micro Energy Harvesters," Journal of Engineering and Applied Sciences (JEAS), Vol. 34, No. 2, pp. 34-46, 2015.
41. Lallart, M., Guyomar, D., Richard, C., and Petit, L., "Nonlinear Optimization of Acoustic Energy Harvesting Using Piezoelectric Devices," The Journal of the Acoustical Society of America, Vol. 128, No. 5, pp. 2739-2748, 2010.
42. Matsuda, T., Tomii, K., Hagiwara, S., Miyake, S., Hasegawa, Y., et al., "Helmholtz Resonator for Lead Zirconate Titanate Acoustic Energy Harvester," Proc. of Journal of Physics: Conference Series, Paper No. 012003, 2013.